

Invariant dynamics in a united-atom model of an ionic liquid

Knudsen, Peter A.; Heyes, David M.; Niss, Kristine; Dini, Daniele; Bailey, Nicholas P.

Published in:
Journal of Chemical Physics

DOI:
[10.1063/5.0177373](https://doi.org/10.1063/5.0177373)

Publication date:
2024

Document Version
Peer reviewed version

Citation for published version (APA):
Knudsen, P. A., Heyes, D. M., Niss, K., Dini, D., & Bailey, N. P. (2024). Invariant dynamics in a united-atom model of an ionic liquid. *Journal of Chemical Physics*, 160(3), Article 034503. <https://doi.org/10.1063/5.0177373>

General rights

Copyright and moral rights for the publications made accessible in the public portal are retained by the authors and/or other copyright owners and it is a condition of accessing publications that users recognise and abide by the legal requirements associated with these rights.

- Users may download and print one copy of any publication from the public portal for the purpose of private study or research.
- You may not further distribute the material or use it for any profit-making activity or commercial gain.
- You may freely distribute the URL identifying the publication in the public portal.

Take down policy

If you believe that this document breaches copyright please contact rucforsk@kb.dk providing details, and we will remove access to the work immediately and investigate your claim.

Invariant dynamics in a united-atom model of an ionic liquid

Peter A. Knudsen,¹ David M. Heyes,² Kristine Niss,¹ Daniele Dini,² and Nicholas P. Bailey^{1, a)}

¹⁾“Glass and Time”, IMFUFA, Dept. of Science and Environment, Roskilde University, P. O. Box 260, DK-4000 Roskilde, Denmark

²⁾Imperial College London, Department of Mechanical Engineering, South Kensington Campus, London SW7 2AZ, UK

(Dated: November 30, 2023)

We study a united-atom model of the ionic liquid 1-butyl-1-methylpyrrolidinium bis(trifluoromethyl)sulfonylamide to determine to what extent there exist curves in the phase diagram along which the microscopic dynamics are invariant when expressed in dimensionless, or reduced, form. The initial identification of these curves, termed isodynes, is made by noting that contours of reduced shear viscosity and reduced self-diffusion coefficient coincide to a good approximation. Choosing specifically the contours of reduced viscosity as nominal isodynes, further simulations were carried out for state points on these, and other aspects of dynamics were investigated to study their degree of invariance. These include the mean-squared displacement, shear-stress autocorrelation function, and various rotational correlation functions. These were invariant to a good approximation, with the main exception being rotations of the anion about its long axis. The dynamical features that are invariant have in common that they are aspects that would be relevant for a coarse-grained description of the system; specifically. Removing the most microscopic degrees of freedom in principle leads to a simplification of the potential energy landscape which allows for the existence of isodynes.

I. INTRODUCTION

The phenomenon of density scaling of dynamics has in the last two decades become an important tool for classifying and understanding the behavior of liquids^{1–3} (although similar approaches have existed for longer⁴). Density scaling refers to the fact that for many liquids, the dependence of many dynamical quantities on thermodynamic variables can be expressed through a particular combination of density ρ and temperature T , specifically

$$X = f(h(\rho)/T), \quad (1)$$

where X is some dynamical quantity, for example a relaxation time, and $h(\rho)$ is a function which depends on the material, and f is a function which is different for different observables. In many cases it can be approximated by a power law, $h(\rho) = \rho^\gamma$, where the so-called density-scaling exponent γ is a material constant. The essence of density scaling can be stated as the dynamical properties are invariant along certain curves in the phase diagram given by $h(\rho)/T = \text{const}$. The realization of its significance was prompted by the rise of high pressure measurements of glass-forming and other complex liquids—the use of an extra parameter allows for a more complete picture of what governs dynamical behavior. The term density scaling usually refers to the finding that the main relaxation time, τ , and the viscosity can be represented as a function of $h(\rho)/T$.^{5,6} In addition to these “scalar” quantities it is also often found that the spectral shape of the relaxation seen for example in dielectric or neutron spectroscopy is invariant along the lines of constant relaxation time.^{1,7–9} This result is called isochronal superposition, but also leads to a generalization of density scaling⁹ (if the relaxation time obeys

density scaling) because it follows that any shape parameter of the spectrum will be a function of $h(\rho)/T$. In other words, for some liquids it is found that the lines in the phase diagram defined by $h(\rho)/T = \text{const}$ have identical dynamics on all time scales and seen in different observables.^{10,11}

A theoretical concept, hidden scale invariance, and a theoretical framework known as isomorph theory, have emerged which can explain density scaling.^{12–14} In fact these lead to a stronger claim, namely that also microscopic structure is invariant on the same curves as dynamics, these curves are now designated as *isomorphs* to emphasize the invariance of structure. The theory specifies how to quantify the degree to which dynamical invariance can be expected and how to identify isomorphs themselves, using methods which are straightforward in computer simulations (at least for the simplest model systems) but less so in experiments. Systems which have good isomorphs are understood to include van der Waals liquids and metals. Typical values of γ for such systems are in the range 4–8 for van der Waals systems (though lower for polymers)¹⁵ and 2–6 for metals.¹⁶ Those systems in which Coulomb interactions dominate, or with strong directional bonds, e.g. in the form of hydrogen bonds, as for example water, do not have good isomorphs in simulations.^{17,18} In experiments there is some evidence that density scaling breaks down for hydrogen bonding systems, particularly when it comes to the spectral shape being invariant over many decades in time and/or at very high (GPa-range) pressures.^{10,19,20} This breakdown is expected from isomorph theory, but it has also been found that some hydrogen bonding systems obey density scaling,^{8,11,21} though possibly in a restricted density range and generally with very low values of γ (around 1).

Ionic liquids are a class of liquids which have received enormous attention in the last two decades, primarily because of their promise in applications.²² They represent also an important category of liquid worthy of study for fundamental reasons: in particular with modern room-temperature ionic liquids, the Coulomb interactions are diluted due to the large size of the molecules. Thus it makes sense to consider them

^{a)}nbailey@ruc.dk

This is the author's peer reviewed, accepted manuscript. However, the online version of record will be different from this version once it has been copyedited and typeset.

PLEASE CITE THIS ARTICLE AS DOI: 10.1063/5.0177373

86 as an intermediate case between van de Waals liquids and¹⁴⁴
87 strongly ionic liquids such as the classical molten salts (e.g.,¹⁴⁵
88 NaCl). There is experimental data demonstrating density scal-¹⁴⁶
89 ing for the different transport coefficients; viscosity, elec-¹⁴⁷
90 trical conductivity and self-diffusion in many different ionic¹⁴⁸
91 liquids.^{23–33} In addition a recent experimental work³⁴ showed¹⁴⁹
92 that the time scale and spectral shape of the main (slow) dy-¹⁵⁰
93 namical process at microscopic scales, seen in neutron spec-¹⁵¹
94 troscopy, are also invariant along the same lines as the con-¹⁵²
95 ductivity for Pyr14TFSI. Moreover these authors also exam-¹⁵³
96 ined the structure factor as measured using X-rays and found¹⁵⁴
97 that it was partly invariant: the so-called charge peak reflect-¹⁵⁵
98 ing charge ordering varied slightly along isoconductivity lines¹⁵⁶
99 while the main peak at large wavenumber was quite invari-¹⁵⁷
100 ant. The density changes involved were small, of order 2%.¹⁵⁸
101 Therefore Pyr14TFSI does not have isomorphs since not all¹⁵⁹
102 of the microscopic structure is invariant, although certain as-¹⁶⁰
103 pects are. If one subscribes to the notion that dynamics and¹⁶¹
104 structure must be related, in that structure, or some particular¹⁶²
105 aspect of it, governs dynamics, then it is not surprising that¹⁶³
106 at least part of the structure is invariant along the isoconduc-¹⁶⁴
107 tivity lines. This reasoning has been called, in the context of¹⁶⁵
108 isomorph theory, the isomorph filter,¹² and a generalized ver-¹⁶⁶
109 sion of it applies here: if one should claim that some aspect¹⁶⁷
110 of structure should "control" the dynamics, then that aspect¹⁶⁸
111 must be invariant along the same curves that dynamics is. If¹⁶⁹
112 one does not know which aspect of structure is controlling the¹⁷⁰
113 dynamics, one should start by searching among those aspects¹⁷¹
114 which are invariant along those lines. In this work we include¹⁷²
115 a limited analysis of structure, and a more detailed discussion¹⁷³
116 can be found in Ref. 35.¹⁷⁴

117 In previous work we studied by simulation a simple model¹⁷⁵
118 of a molten salt³⁶ over a large density range. The wide range¹⁷⁶
119 allowed us to effectively vary the strength of the Coulomb in-¹⁷⁷
120 teractions: at high densities they become less relevant com-¹⁷⁸
121 pared to the other interactions, due to the relatively slow rise¹⁷⁹
122 of the Coulomb potential at short distances. In that work dy-¹⁸⁰
123 namics and structure were studied along curves of constant¹⁸¹
124 excess entropy, which according to isomorph theory are iso-¹⁸²
125 morphs, assuming these exist.^{12,37} Curves of constant excess¹⁸³
126 entropy—which always exist—are referred to as configurational¹⁸⁴
127 adiabats. A remarkable contrast was revealed, between dy-¹⁸⁵
128 namic invariance along configurational adiabats on one hand,¹⁸⁶
129 and substantial variation of structure on the other hand. When¹⁸⁷
130 restricting to moderate density changes and considering the¹⁸⁸
131 structure factor, a similar picture to that reported by Hansen *et*¹⁸⁹
132 *al.* was found, namely a near invariance of the main peak to-¹⁹⁰
133 gether with a variation in the charge peak. But the larger pic-¹⁹¹
134 ture can be expressed as the contrast between near-invariant¹⁹²
135 dynamics and non-invariant structure. This contrast was strik-¹⁹³
136 ing enough to justify coining new terminology: we desig-¹⁹⁴
137 nated curves along which dynamics are invariant as *isodynes*.¹⁹⁵
138 Clearly by this definition isomorphs are isodynes, but the re-¹⁹⁶
139 verse is not true in general, as has become evident also in¹⁹⁷
140 some recent publications.^{38–40} We note that early simulation¹⁹⁸
141 work on density scaling in charged systems seemed to indicate¹⁹⁹
142 that the presence of charges prevented good density scaling,⁴¹²⁰⁰
143 although only power-law density scaling was attempted, and²⁰¹

the charges were rather large in that case. Our 2021 work on
the simple molten salt shows that a regime exists where the
charges are strong enough to have non-trivial effects but good
isodynes can nevertheless be observed. On a related matter
it has proved difficult to establish corresponding states equa-
tions for molten salts because the van der Waals and electro-
static terms in the potential are not mutually scalable in the
same way,⁴² although recent works have studied the appli-
cability of entropy scaling for simple monovalent salts⁴³ and
ionic liquids.⁴⁴

In the absence of isomorphs, we lack a theoretical founda-
tion to explain the existence of isodynes, which is in fact rather
puzzling and an open question. In simple liquids it is likely
related to the phenomenon of excess-entropy scaling.^{45,46} For
more complex molecular liquids, the answer will presumably
somehow involve understanding in a coarse-grained sense
which aspects of the microscopic structure are actually rel-
evant for the dynamics of interest;⁴⁷ but the question stands
also for the simple molten salt model studied in our previous
work, where coarse graining would not seem to be a relevant
strategy. In addition, there is no theoretical ground for assum-
ing any particular scaling form: the argument of the function
 f in Eq. (1) is not required to have the form $h(\rho)/T$, but could
have for example the form $\rho/h'(T)$, as we shall see later. The
approach taken in this work is therefore to focus on identify-
ing curves of invariant dynamics. Whether a suitable scaling
variable can be identified for a density scaling analysis is an
interesting, but separate question.

The purpose of this work is to study by simulation a real-
istic model of an ionic liquid which has been demonstrated to
have isodynes experimentally. If the simulated system like-
wise has isodynes it offers the possibility to study these iso-
dynes in much more detail than what can be done experimen-
tally. The specific aim is thus (1) to determine to what extent
isodynes exist in the simulated ionic liquid, (2) to character-
ize their shape in the phase diagram, in particular the value(s)
of the density scaling exponent γ , and (3) to document which
aspects of microscopic dynamics are indeed invariant along
the identified isodynes. The strategy is as follows. For item
1, we focus initially on the viscosity and the diffusion coef-
ficient(s). Comparing contour plots of these quantities (ap-
propriately scaled, what we refer to below as "reduced units")
will give the first indications of isodynes. A series of simula-
tions along putative isodynes chosen as for example viscosity
contours allows direct checks of invariance of other quantities,
including orientational dynamics.

The system we investigate in this work has
the full name 1-butyl-1-methylpyrrolidinium
bis(trifluoromethyl)sulfonylamide. We abbreviate the
cation as Pyr14; it has a molar mass of 142.257 g/mol and is
also referred to in the literature as C₄MPYRR (the M standing
for methyl). The anion, which we abbreviate as TFSI, has a
molar mass of 280.143 g/mol, and is also referred to in the
literature as NTF₂. The total molar mass is thus 422.4 g/mol.
Both ions have appeared in many studies on ILs, the cation
often as part of a series Pyr1 n where n , equal to four in our
case, is the number of carbon units on the tail. The cation
and anion are shown schematically in Fig. 1. Pyrrolidinium

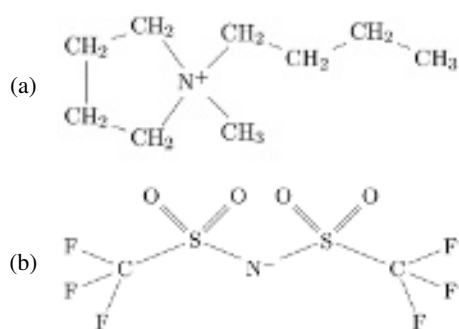


Figure 1. Visual representation of the molecular structures of the (a) cation, 1-butyl-1-methylpyrrolidinium (Pyr14) and (b) anion, bis(trifluoromethyl)sulfonylamide (TFSI), simulated in this work.

This is the author's peer reviewed, accepted manuscript. However, the online version of record will be different from this version once it has been copyedited and typeset. PLEASE CITE THIS ARTICLE AS DOI: 10.1063/5.0177373

ILs are used in electrochemical applications because of their wide electrochemical windows and high electrochemical stabilities.²² The structure of the paper is as follows. Sec. II gives details of the liquid to be studied, and of the simulation model and potential. Sec. III gives an overview of the simulations and includes some comparisons with experimental data. In Sec. IV we present our procedure for identifying isodynes and describe our main results, namely the presentation of dynamical data of along different isodynes. Sec. V discusses the significance of the results in terms of the larger question of how widespread isodynes are. It also discusses how the concept of coarse-graining is connected to the existence of isodynes in complex molecular systems. Section VI offers some perspectives for future work.

II. MODEL AND POTENTIAL

For most of our results we use a united-atom model for the Pyr14 cation, i.e. representing each CH₂ or CH₃ group as a single sphere in order to reduce the number of degrees of freedom and to increase the time step (due to not having to resolve the CH bond vibration). There are no H atoms on TFSI, so there is no possible simplification by using united atoms there. Comparison between all-atom and united-atom models shows that the latter tends to be less viscous, in general, with viscosities typically lower by factors 2-3, than the corresponding all-atom models.⁴⁸ This does not mean that the all-atom viscosity is necessarily closer to experimental values, however, and force field parameters should always be selected to provide the most accurate representation of densities and viscosities for the system under consideration.

We use literature parameters coming from the OPLS family of all-atom molecular force fields⁴⁹⁻⁵¹ which we have adapted as necessary to our UA model. The increased interest in ionic liquids has also led to the development of OPLS extensions for this class of liquids^{52,53}. For our system the earliest set of OPLS parameters for the anion (TFSI) we have found is in Ref. 54, which provides all non-bonded interactions (including partial charges) and all bonded interactions (bonds, angles,

and dihedrals). For our cation (Pyr₁₄) we used the parameters from Xing et al.⁵⁵ who used standard bonded and non-bonded parameters from Refs. 56 and 57. Furthermore Xing et al.⁵⁵ obtained the partial charges from the optimized geometry using the RESP method with the R.E.D.-III.4 package. We have adapted these all-atom literature parameters to make corresponding united-atom potentials. To make a united-atom model of the molecule we replace the CH₂ and CH₃ groups in Pyr₁₄ with Lennard-Jones spheres, with the non-bonded parameters for these taken from Refs. 58 and 59. The partial charges of the united atoms are simply the total charge of the relevant C and H atoms. To account for polarizability effects in a simple way we scale all partial charges by a factor 0.8;⁵³ this is discussed in the Supplemental Material. We use the unit system where lengths are in Angstrom (Å), energies are in kcal/mol, masses are in dalton (u), and charges in units of the elementary charge (*e*). Molecular number densities (total number of ions per unit volume) are expressed in nm⁻³ rather than Å⁻³ for convenience, however.

Some technical differences from the usual OPLS implementations should be noted. The interactions are truncated via the shifted-force method, and is applied at 2.5σ for each interaction, rather than having a common absolute cutoff distance. We also use this cutoff method for the electrostatic (Coulomb) interactions, omitting the long-range part of these (see the Supplemental Material). Secondly, we use Lorentz-Bertholot mixing rules rather than purely geometric rules as is standard with OPLS potentials. Finally we exclude non-bonding interactions for all atoms involved in a dihedral interaction, rather than applying a 0.5 weighting for the extreme atoms (1 and 4) as is standard in OPLS. The differences presumably have some effect on the pressure (and possibly the bulk modulus), meaning it is wise to be cautious in comparing the simulation-derived pressures with experimental data. While the choice of mixing rules has been shown to have an effect on solubility of NaCl in water⁶⁰, such effects are not expected to be relevant or significant in the present case. All simulations in this work were performed with *Roskilde University Molecular Dynamics* (RUMD), Version 3.5.⁶¹ We have carried out a limited number of simulations using an all-atom model. The most interesting question here is whether isodynes of the united-atom model are also isodynes in the AA-model, which can be determined by simulating the AA model on state points identified as being on an isodynes of the UA model.

III. SIMULATIONS

A. Simulated region of the phase diagram

Figure 2 shows the part of density temperature phase diagram we have simulated. The overall region of interest in the phase diagram can be defined by three criteria which are: (1) requiring positive pressure, which defines a boundary with a negative slope on the low-density side, close to the liquid-gas coexistence curve, the region thus excluded being colored grey; (2) relaxation times accessible to simulation, allowing the determination of equilibrium properties within reasonable

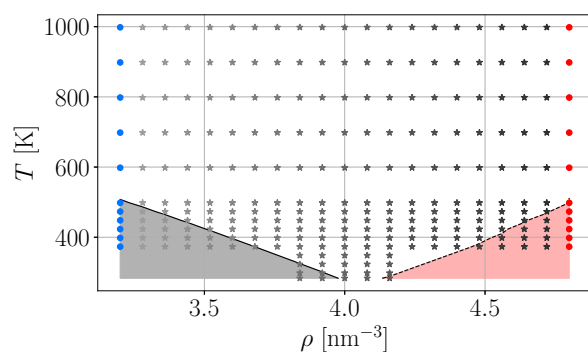


Figure 2. Density-temperature phase diagram showing simulated points. The boundary curve on the lower left represents zero pressure and that on the lower right represents impractically slow dynamics, determined by the criterion that it takes 1 ns for the self-intermediate scattering function of N^+ to reach a value of e^{-1} . The q in the self-intermediate scattering function was chosen to be the position of the main structure factor peak. For our simulations it is between 0.7 and 0.9 \AA^{-1} .

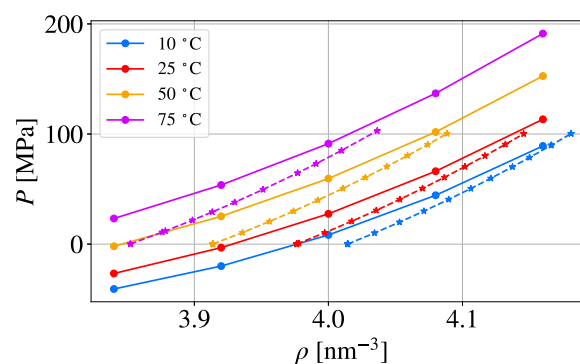


Figure 3. Simulated pressure-density isotherms (dots, solid lines) compared with experimental data of Harris et al.⁶⁴ (stars, dashed lines). Statistical errors on the simulation data have been estimated using standard methods, determining the number of independent samples based on the time taken for the pressure autocorrelation to fall below 5% of its initial value. The errors are of order 0.5 MPa, and in all cases smaller than the symbol size.

This is the author's peer reviewed, accepted manuscript. However, the online version of record will be different from this version once it has been copyedited and typeset.

PLEASE CITE THIS ARTICLE AS DOI: 10.1063/5.0177373

294 times, which defines a boundary with positive slope on the 327
 295 high-density side, corresponding to a version of the glass tran-328
 296 sition line, the region excluded being coloured red; and (3) 329
 297 an upper temperature limit, in principle corresponding to the 330
 298 limit of thermal stability of the molecules. For criterion (1) 331
 299 we use the uncorrected pressure of the model; we estimated 332
 300 the corrected pressure would be about 10 MPa lower due to 333
 301 the long-range part of the Coulomb interaction (though there 334
 302 are other uncertainties in the pressure), such that the zero-335
 303 pressure line would exclude a greater part of the phase dia-336
 304 gram. For criterion (2) we define a timescale τ_{F_s} from the 337
 305 self-intermediate scattering function curve (F_s) for the N-atom 338
 306 on the cation (N^+), as the time at which the F_s reaches a value 339
 307 of e^{-1} of its initial value. The criterion in the phase diagram 340
 308 is that $\tau_{F_s} = 1$ ns. Regarding criterion (3), thermal stability of 341
 309 ionic liquids has been extensively studied; the so-called onset 342
 310 temperature (at ambient) pressure is typically between 450 K 343
 311 and 750 K⁶². For our liquid the onset temperature has been 344
 312 measured at 724 K⁶². Given that our model cannot decompose 345
 313 thermally anyway, we choose to extend this limit somewhat, 346
 314 up to 1000 K; studying it over a broader temperature range 347
 315 allows us get a clearer idea of its overall behavior. For orien- 348
 316 tation, we note that the critical point has been estimated for 349
 317 this IL to be around density 0.57 nm^{-3} and temperature 1050 350
 318 K,⁶³ thus well to the left and at higher temperature than the 351
 319 points shown. 352

320 B. Comparison with experiment: equation of state and 355 321 viscosity 356

322 To find how well the model resembles reality we compare 358
 323 pressure, diffusion coefficient and viscosity with experimental 359
 324 data from Harris et al.⁶⁴ The diffusion coefficient data was 360
 325 only provided as a function of pressure; given the systematic 361
 326 uncertainties in the simulated pressure discussed above, for 362

comparison we determined the experimental densities using the equation of state from Ref. 34, where the Tait equation was used. A consistency check with data in Ref. 64 shows that the uncertainty on the determined experimental densities is of order 0.3%. Thus we can plot instead the experimental data together with the simulation data as a function of density on isotherms.

To assess the systematic errors in our simulated pressure we compare it with the experimental data, see fig. 3. Our simulated pressures are generally greater than the experimental ones, by up to 20 MPa, when comparing data at equal temperature; the overall pressure range of our simulated data is comparable with that of the experimental data, however. The simulated slopes are smaller than the experimental ones, indicating a bulk modulus roughly 10-20% smaller. These discrepancies are at least partly due to the cutoff, not least regarding the long-range part of the Coulomb interactions. It is possible that the curves converge (rather than cross) at even higher densities, meaning that the missing part of the pressure becomes less important at higher densities.

When comparing the diffusion coefficient we consider the two isotherms $T = 50^\circ\text{C}$ and 75°C , see Fig. 4 (a). The simulated and experimental data are in a similar range, with the simulations generally being faster (by factors of order 1.5-2). The deviation is larger for the lower temperature. The data are nearly exponential in density, with remarkably similar slopes in the semi-log representation, differing only by a few percent both between isotherms and between experiment and model.

Fig. 4 (b) shows the comparison of the viscosity between the simulations and experiments. As before experimental and simulated values are comparable, with the simulated viscosity being lower by factors up to 3. Considering data for 50°C and 75°C , the discrepancies are quite similar to those for the diffusion coefficient, indicating that the simulated liquid's dynamics are overall faster by factors of order 2 and 1.5 than the corresponding experimental system, respectively for these

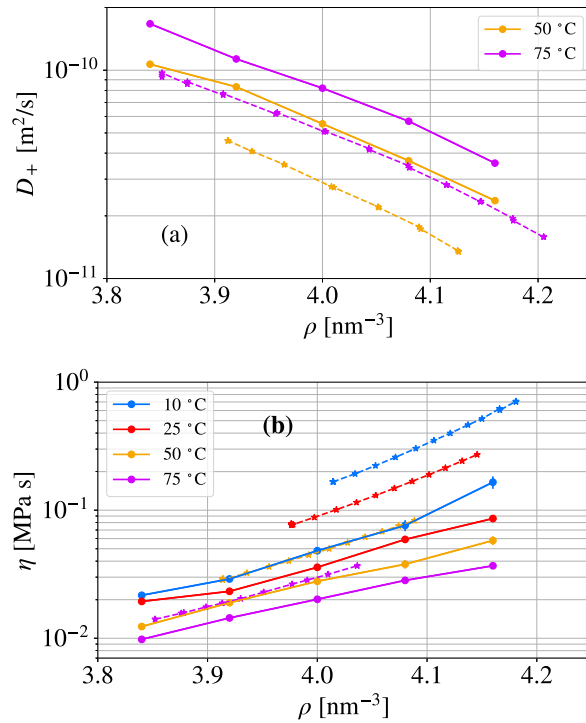


Figure 4. Simulated transport coefficients (dots, solid lines) compared with experimental data of Harris et al.⁶⁴ (stars, dashed lines) (a) Diffusion coefficients of the cation D_+ as a function of ρ . (b) η as a function of ρ .

363 temperatures. Moreover it is clear also here that the discrepan-
 364 cy grows as temperature decreases to even lower values,
 365 while the density dependence is remarkably similar across
 366 temperatures and between experiment and model. The combi-
 367 nation of differences and similarities has consequences for
 368 the density scaling exponent, as will be discussed below.

369 IV. DYNAMICS AND ISODYNES

370 A. Reduced units

371 In our earlier study³⁶ we used isomorph theory to anal-
 372 yse the simple salt model of Hansen and McDonald⁶⁵. We
 373 found lines in the $\rho - T$ phase diagram where the dynamics³⁸⁶
 374 are invariant when scaled according to the isomorph theory.³⁸⁷
 375 This scaling, introduced by Rosenfeld,⁶⁶ uses thermodynamic
 376 properties such as number density ρ and temperature T so³⁸⁸
 377 that the scaled quantity becomes dimensionless. These re-³⁸⁹
 378 duced quantities are symbolized by a tilde. Thus, a distance³⁹⁰
 379 r in reduced units becomes $\tilde{r} = \rho^{1/3}r$. The three fundamental³⁹¹
 380 scaling factors, along with two derived ones, can be found in³⁹²
 381 Table. I. A more detailed list of scaling factors for isomorph³⁹³
 382 scaling may be found in Gnan et al.¹² The same scaling of³⁹⁴
 383 quantities to make them non-dimensional has been used by³⁹⁵
 384 Dymond et al., who were inspired by a hard-sphere-type mod-³⁹⁶
 385 elling scheme; see for example Refs. 4 and 67. 397

Dimension	Scaling factor	Reduced quantity
Length	$l_0 = \rho^{-1/3}$	$\tilde{l} = l/l_0$
Energy	$E_0 = k_B T$	$\tilde{E} = E/E_0$
Time	$t_0 = \rho^{-1/3} \sqrt{\frac{m}{k_B T}}$	$\tilde{t} = t/t_0$
Diffusivity	l_0^2/t_0	$\tilde{D} = D\rho^{1/3}(k_B T/m)^{-1/2}$
Viscosity	$E_0 t_0/l_0^3$	$\tilde{\eta} = \eta\rho^{-2/3}(mk_B T)^{-1/2}$

Table I. List of scaling factors for isomorph scaling. The first three, energy, length and time can be considered fundamental (alternatively mass can be taken as fundamental); all others can be derived from these three essentially by dimensional analysis.

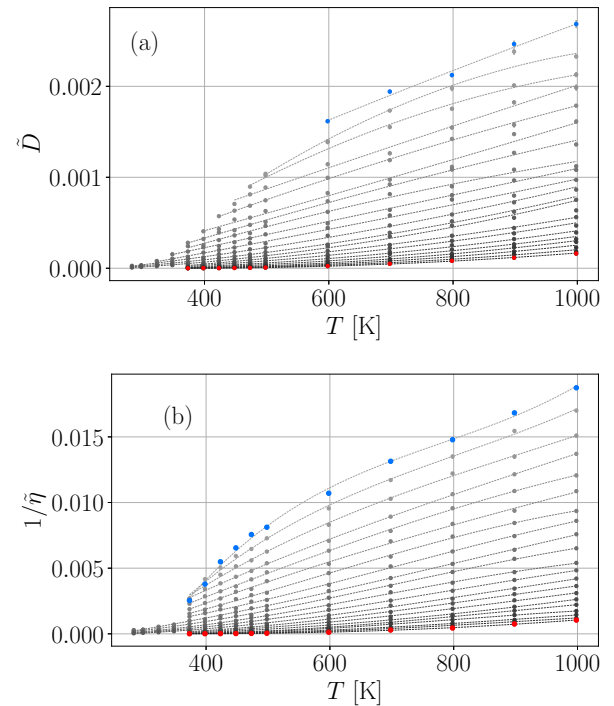


Figure 5. Fits of (a) reduced diffusion coefficient for cations (specifically the N^+ atom) \tilde{D} , and fits to second-order polynomial and (b) the fluidity, or inverse viscosity $1/\tilde{\eta}$, as a function of temperature for different densities, together with fits to third-order polynomial. Colors correspond also to the points shown in Fig. 2. Data for the lowest and highest densities are plotted in blue and red, respectively (see Fig. 2).

B. Determining isodynes using viscosity and diffusion coefficient

Figure 5 shows our data for the cation diffusion coefficient and the inverse viscosity (also known as the fluidity). Fits to second and third-order polynomials, as a function of temperature for each simulated density, are also shown. The diffusivity data include more scatter, and a third order polynomial was observed to overfit the data. The reason for the scatter is likely the relative small number (200) of cations in the simulation, leading to statistics that are poorer than usual for simulated liquids. These fits were obtained primarily for the purpose of interpolation so that contours of \tilde{D} and $\tilde{\eta}$ could be identified.

This is the author's peer reviewed, accepted manuscript. However, the online version of record will be different from this version once it has been copyedited and typeset.

PLEASE CITE THIS ARTICLE AS DOI: 10.1063/5.0177373

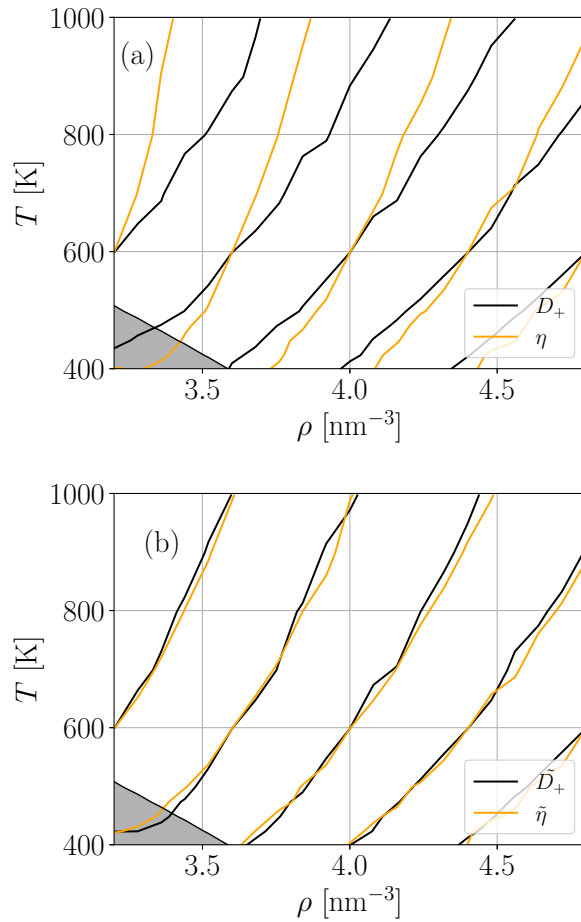


Figure 6. Contours of diffusivity and shear viscosity in the ρ - T diagram in (a) standard units and (b) reduced units. The contours were chosen to pass through the following points: $\rho = 3.2; 3.6; 4.0; 4.4; 4.8 \text{ nm}^{-3}$, all at $T = 598.15 \text{ K}$.

398 Contour plots showing selected contours of D and η are
 399 shown in Fig. 6(a), while contours of the reduced quantities \tilde{D}
 400 and $\tilde{\eta}$ are given in Fig. 6(b). These plots were generated from
 401 a grid of values using a standard algorithm.⁶⁸ The contour-
 402 values have been chosen to make approximately coincident
 403 contours of the two quantities at $T = 598 \text{ K}$. It is clear that the
 404 two sets of contours for the nonreduced quantities do not coin-
 405 cide, while those for the reduced quantities match remarkably
 406 well. The black curves (diffusivity) appear to be systemati-
 407 cally slightly steeper, though this difference is barely larger
 408 than the apparent noise. Therefore we can identify these com-
 409 mon contours as *isodynes* or curves of invariant dynamics (in
 410 reduced units).

411 For further investigation we choose specifically to work
 412 with contours of reduced viscosity to generate isodynes. New
 413 simulations were then run at densities and temperatures along
 414 several different isodynes. For generating these contours of
 415 reduced viscosity we rely on the fits shown in Fig. 5. For
 416 a given value of reduced viscosity (or inverse reduced vis-
 417 cosity) and for each density, the corresponding temperature

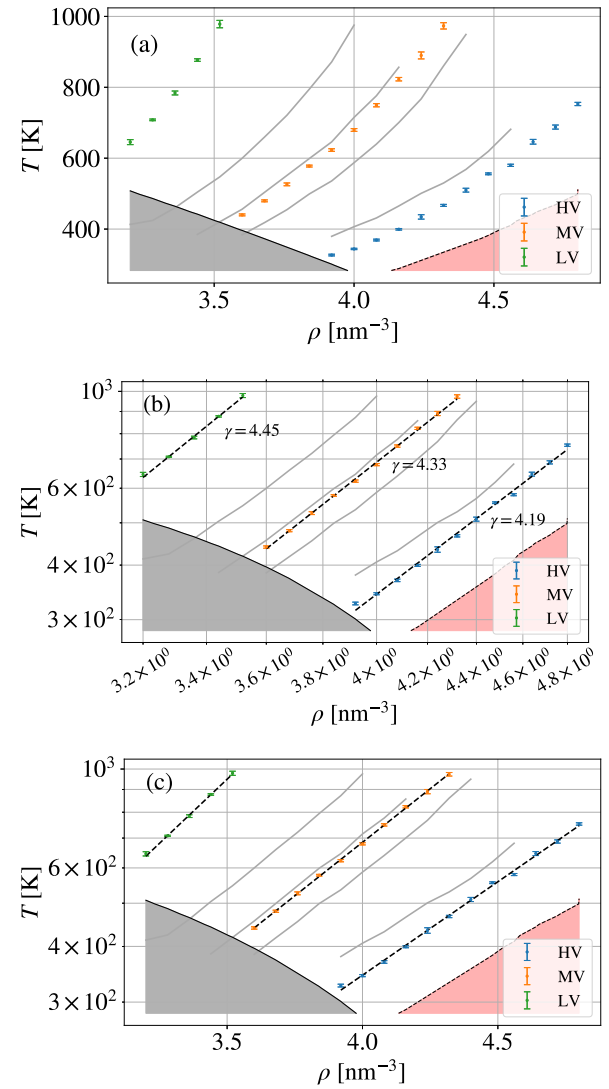


Figure 7. Selected isodynes shown in (a) lin-lin (b) log-log and (c) log-lin plots. Power-law and exponential fits are included in (b) and (c), respectively. The colored points indicated the three isodynes HV ($\tilde{\eta} = 0.01188$), MV ($\tilde{\eta} = 0.00297$) and LV ($\tilde{\eta} = 0.00037$) that we focus on in the analysis, while the grey ones indicate other isodynes on which simulations have been run. For the power-law fits the values of the density scaling exponent γ are shown by each curve.

was found by interpolation. The covariance matrix from the polynomial fits was used to construct error bars for the temperature. In the analysis below we focus primarily on three isodynes, labelled HV, MV and LV for high, medium and low (reduced) viscosity, respectively, and chosen to cover a broad region of the phase diagram. The other isodynes that have been simulated are shown in grey in the figures. Before presenting simulation data along the isodynes we discuss their shapes in the next subsection and discuss the relevance of the Stokes-Einstein relation to isodynes in the following subsection.

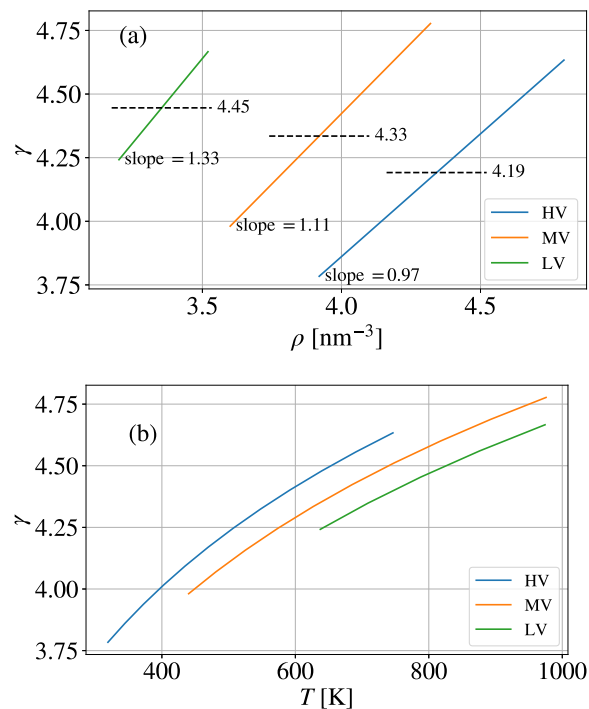


Figure 8. Density scaling exponent γ from exponential fits to isodynes plotted as function of (a) ρ and (b) T . The values of the b parameter are indicated in the figure. The values of the parameter T_0 were 7.26, 8.22, 9.16 for HV, MV and LV, respectively.

C. The shape of isodynes

The existence of common invariant curves for two (or more) different dynamical quantities does not by itself imply the scaling form Eq. (1)—that has to be determined from analysis of their shapes. Fig. 7(a), (b) and (c) show selected isodynes on linear, double logarithmic and semi-logarithmic scales, respectively. In panel (b) power-law fits are included, with the exponents γ indicated. The γ values are in the fairly narrow range 4.3–4.4, seemingly higher for higher temperatures and lower densities. Alternatively the contours can be fitted using exponential functions,

$$T(\rho) = T_0 \exp(b\rho); \quad (2)$$

the density scaling exponent γ is then no longer constant along a given isodyne but is defined as the logarithmic derivative

$$\gamma(\rho) \equiv \frac{d \ln h(\rho)}{d \ln \rho} = b\rho = \ln \left(\frac{T}{T_0} \right). \quad (3)$$

The exponential fits are shown in Fig. 7(c). They are slightly better than the power-law fits (around a factor of two reduction in χ^2). Apart from fitting the isodynes better, the exponential fits give a more complete picture of how γ varies in the phase diagram. Along a given isodyne one can express γ as a function of either ρ or T as indicated in Eq. (3). But γ can be

defined at any point in the ρ, T -plane as the logarithmic slope of whichever isodyne passes through that point, and in general is a function of both ρ and T . We can get a sense of how much γ depends primarily either on ρ or T by plotting the fitted values of γ as a function of each separately. Fig. 8(a) and (b) show plots of γ versus density for each isodyne versus ρ and T , respectively. Greater variation of γ overall is apparent than was seen in the power-law fits, covering values between 3.8 to 4.8 (the constant values of γ from the power-law fits are also shown in Fig. 8(a) for comparison). Moreover it is clear from the approximate collapse visible in Fig. 8(b) that γ depends primarily on T and relatively little on ρ if T is held fixed. In terms of the fit parameters T_0 and b from the exponential fit, this means that T_0 depends rather little on which isodyne is considered while b varies significantly.

The experimental density scaling exponent for this system was determined to have significantly lower values, in the range 2.8–3.0,³⁴ than what we see. Some of the difference can be explained by the lower temperatures in the experimental measurements (< 310 K), but no reasonable extrapolation of the blue curve, say, will take γ down to 3 at $T = 300$ K. The greater values of γ in the model are, however, consistent with the observations made above in comparing experimental and simulated data for the diffusion coefficient and viscosity (see Sec. III B, Fig. 4). There it was noted that the density dependence was rather uniform, both across different isotherms and between experimental and simulated data, while the temperature dependence differs between experiment and model. In particular, the viscosity increases more rapidly upon cooling at fixed density for the experimental system than for the model. This is equivalent to a smaller γ for the experimental case by the following argument: for a given ρ, T starting point, a given increase in ρ increases both the experimental and model (reduced) viscosity by the same fractional amount. To compensate for this and return to the starting contour the temperature must be decreased. Because the experimental system is more sensitive to temperature (at fixed density), a smaller temperature change is required, corresponding to a smaller γ . This reasoning makes use of the fact that a given increase in density gives essentially the same factor increase in viscosity in both the real and the model systems.

D. Density scaling analysis

The concept of isodynes is closely related to that of density scaling, as mentioned in the introduction. Traditionally density scaling has been illustrated by plotting the putative invariant quantity as a function of some scaling variable Γ . For the simplest case, $\Gamma = \rho^{\gamma_0}/T$, corresponding to power-law isodynes $T \propto \rho^{\gamma_0}$ (the subscript 0 on γ is to emphasize that this is a fixed parameter). For an expression which can account for the variation of γ with temperature we can use the exponential fits from above, recalling that the parameter T_0 was relatively insensitive to the choice of isodyne. Taking the last expression for γ in Eq. (3) as a general expression for $\gamma(\rho, T)$,

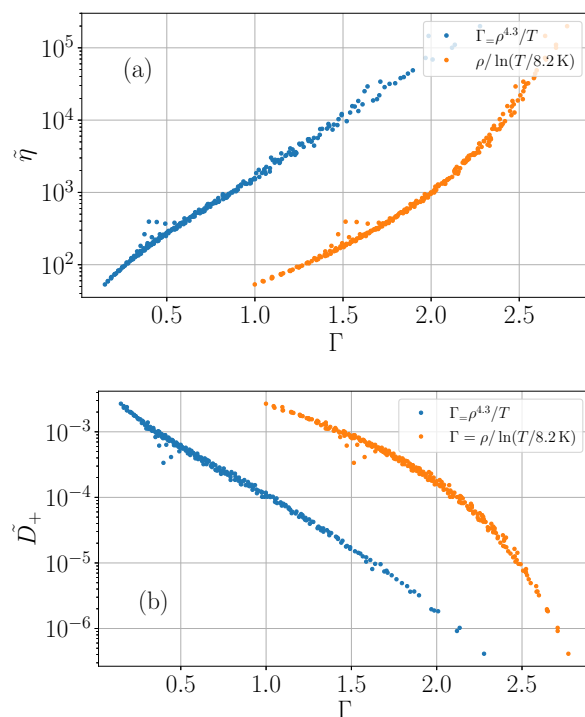


Figure 9. Density scaling plot for (a) reduced viscosity and (b) cation diffusivity. Two choices of scaling variable Γ are used (see Eq. (5)): one corresponding to ordinary density scaling ($\Gamma = \rho^{\gamma_0}/T$) and one corresponding to the T -dependent γ , namely $\Gamma = \rho/\ln(T/T_0)$, with T_0 to be 8.2 K from the parameters for the middle curve in Fig. 8. What is plotted is actually $3\Gamma - 1$ to spread the data out in the x-axis to make it easier to compare the degree of collapse in the two cases.

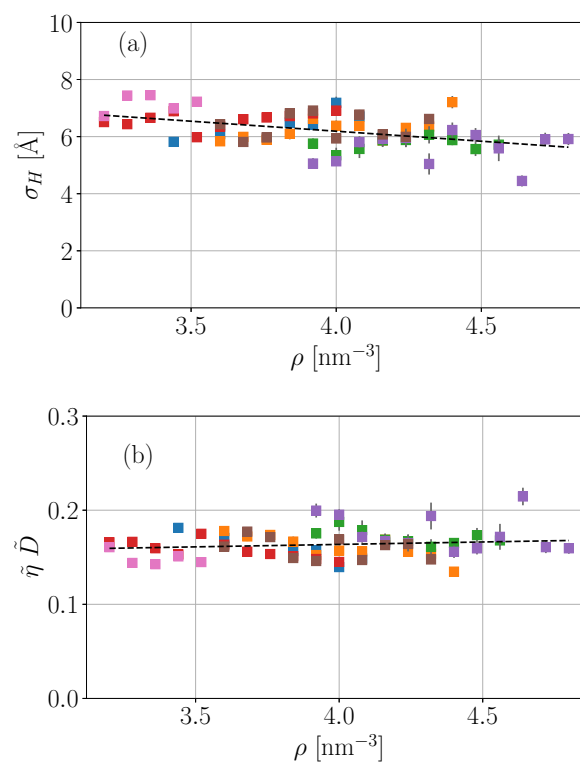


Figure 10. Test of the Stokes-Einstein relation, data from the simulated isodynes. (a) Effective hydrodynamic diameter, (b) the dimensionless quantity $\tilde{\eta}\tilde{D}$ which is involved in the isomorph-compatible version of the reduced Stokes-Einstein relation. The colors indicate points on different isodynes.

$$\gamma(\rho, T) = \ln\left(\frac{T}{T_0}\right), \quad (4)$$

gives isodynes with the form Eq. (2), with a common value of T_0 but different values of b . The latter, or more conveniently, its reciprocal, is therefore a natural choice of scaling variable (an index which can distinguish different isodynes) and can be expressed in terms of ρ and T as

$$\Gamma \equiv b^{-1} = \frac{\rho}{\ln(T/T_0)}. \quad (5)$$

The parameter T_0 is in this formulation a characteristic temperature for the material. Fig. 9 shows density scaling plots for reduced viscosity and reduced diffusivity, respectively. The state points used here are those plotted in Fig. 2, i.e. the grid of points used for the initial simulations from which isodynes were identified. In each case the blue points show the case of power-law density scaling and we have chosen $\gamma_0 = 4.3$ as a representative value from the middle of the region of interest (Fig. 8 (a)). The orange points show the choice $\Gamma = \rho/\ln(T/T_0)$ with $T_0 = 8.2$ K, based on the fit to the middle curve (MV) in Fig. 8. Both choices give reasonably sim-

ilar scaling collapses of the data. This shows that smaller errors are required to be able to conclude anything about γ and its temperature or density dependence using a density-scaling analysis.

The weak (i.e. logarithmic here) temperature dependence of γ as evident in Eq. (3) may be a generic feature of ionic liquids. Molten salts are often referred to as being high temperature liquids for obvious reasons. However, in regard to their physical properties they are perhaps better described as being ‘low temperature’ liquids in a statistical mechanical sense as $k_B T/\epsilon \ll 1$ where ϵ is the well-depth at contact of the excluded volumes because of the very large magnitude of the Coulomb energy in units of ambient values of $k_B T$ at typical charge separations in the system. This is illustrated by, for example, the very low value of the critical temperature ($T_c^* \simeq 0.05$) of the Restricted Primitive Model (RPM) of an ionic liquid.⁶⁹ This might lead one to conclude that the Coulombic terms in ionic liquids might be treatable for practical purposes as a uniform background which just shifts the macroscopic unit collapse curves, and that the basic transport coefficient expressions found for neutral polyatomic liquids (e.g., by Dymond *et al.*) might also apply to a large extent to the present systems, as may be inferred from the data trends in Fig. 9.

541 E. Stokes-Einstein relation

542 Diffusivity and viscosity are often assumed to be related
543 through the so-called Stokes-Einstein (SE) relation,⁷⁰ and de-
544 viations from it are considered noteworthy, as in the case of
545 several IL simulations.^{71–74} It is therefore important to investi-
546 gate to what extent the SE relation is compatible with the ex-
547 istence of isodynes. The connection between the SE relation
548 and isomorph theory has been explored recently and suggests
549 a reformulation of the SE relation.⁷⁵ To test the standard SE
550 relation, Fig. 10(a) shows the effective hydrodynamic diam-
551 eter,

$$\sigma_H = \frac{k_B T}{2\pi D \eta}, \quad (6)$$

552 for state points on all simulated isodynes (the coefficient 2 in
553 the denominator applying for slip boundary conditions). The
554 value of σ_H be constant if the standard Stokes-Einstein rela-
555 tion were strictly valid, as for a macroscopic hard sphere dif-
556 fusing in a viscous liquid. Here the hydrodynamic diameter is
557 seen to decrease, albeit weakly, with increasing density.

558 A modification of the original Stokes-Einstein relationship
559 at the microscopic scale,⁷⁰ was made by Zwanzig, who de-
560 rived a hydrodynamic diameter given by $\rho^{-1/3}$, using a semi-
561 empirical quasi-lattice model for the dynamics of the liq-
562 uid molecules,^{76–79} following earlier works.^{80,81} The Zwanzig
563 version of the SE formula is given by the identity, $\tilde{\eta} \tilde{D} = \text{const.}$
564 The same conclusion was made by Costigliola *et al.*,⁷⁵ who
565 noted that this formulation is more compatible with isomorph
566 theory. Indeed, the Stokes-Einstein (SE) relationship written
567 in isomorph (reduced) units is,

$$\begin{aligned} \tilde{D} \tilde{\eta} &= \frac{1}{c\pi \tilde{\sigma}_H}, \\ \tilde{D} \tilde{\eta} &= \alpha = \frac{1}{c\pi}, \quad \text{if } \tilde{\sigma}_H = 1 \end{aligned} \quad (7)$$

568 where the characteristic diameter is, $\tilde{\sigma}_H = \sigma_H \rho^{1/3}$. The con-
569 stants, $c = 2$ and 3 correspond to slip and stick boundary con-
570 ditions. Thus the SE constant $\alpha = 1/c\pi = 0.159$ and 0.106
571 for slip and stick boundary conditions, respectively, where
572 $\tilde{\sigma}_H = 1$ at all state points is taken (i.e., the Zwanzig result).
573 Note that in Eq. (7) when the SE is expressed in isomorph
574 units, it is evident that there is no temperature dependence of
575 the SE constant, α .

576 Fig. 10 (b) shows the dimensionless quantity $\alpha = \tilde{\eta} \tilde{D}$. It
577 is clear that this is a better candidate for an invariant quantity
578 reflecting molecular dynamics in the framework of isomorph
579 theory⁷⁵. Isomorph theory does not require α to be constant
580 but it can be collapsed as a function of temperature on a sin-
581 gle curve. At low to moderate temperatures α approaches a
582 constant value, which for the Lennard-Jones (LJ) fluid for ex-
583 ample is observed to be 0.146 .⁷⁵ Values of α at high density
584 are *ca.* 0.15 for LJ, 0.17 for hard spheres, and 0.14 for the one-
585 component plasma and Yukawa ($\kappa = 2$) potential systems,^{82,607}
586 and for TIP4/ice water, $\alpha = 0.15 \pm 0.02$.⁸³ Our data is consis-
587 tent with a constant value in the range 0.15 - 0.20 , and therefore

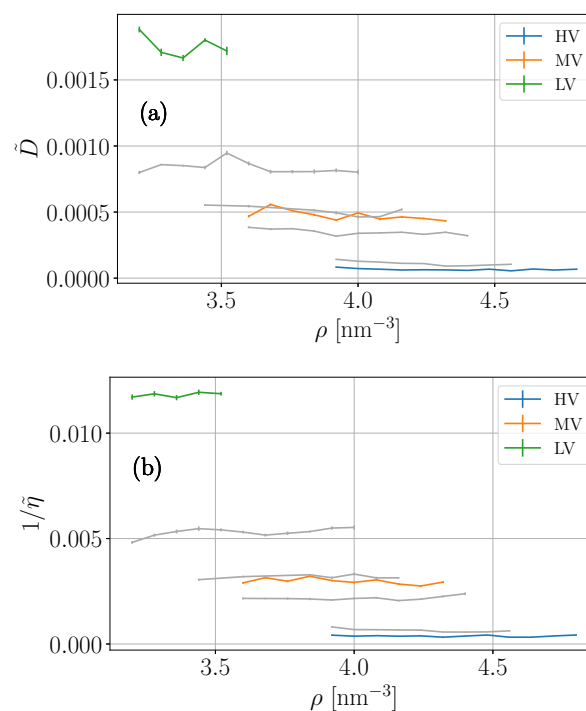


Figure 11. Dynamics along all simulated isodynes in scaled units. The colored ones are the three main simulated isodynes we have focused on. The grey ones are other isodynes we simulated but have not studied in detail. They are included here as extra checks that our procedure yields reasonably invariant dynamics along isodynes. (a) Scaled diffusion coefficient for N^+ in the cation, and (b) scaled inverse viscosity (fluidity).

588 consistent with these other studies on model systems, and the
589 results of Costigliola *et al.*⁷⁵, suggesting the possibility that
590 this quantity is largely invariant across a range of different
591 chemical systems.

592 The physical content of the "isomorph-compatible", or the
593 Zwanzig version of the Stokes-Einstein relation is that the ef-
594 fective hydrodynamic diameter refers not to a fixed molecular
595 size, but rather to the space available for a molecule to oc-
596 cupy, which is determined by the density. The existence of
597 isodynes implies that $\tilde{\eta} \tilde{D}$ is constant along any given isodyne,
598 but by itself does not imply that the constant is independent
599 of which isodyne is considered. Thus the collapse to a sin-
600 gle value (within the simulation statistics), which is consis-
601 tent with the isomorph version of the SE relation, is a stronger
602 result.

F. Simulations along proposed isodynes

In this and the following subsections data from simulations carried out on the proposed isodynes are presented. The isodynes were identified as described in subsection IV B.

The viscosity, self-diffusion coefficient and other dynamical quantities are investigated to discover the extent to which they exhibit invariant dynamics. Figure 11 shows the values

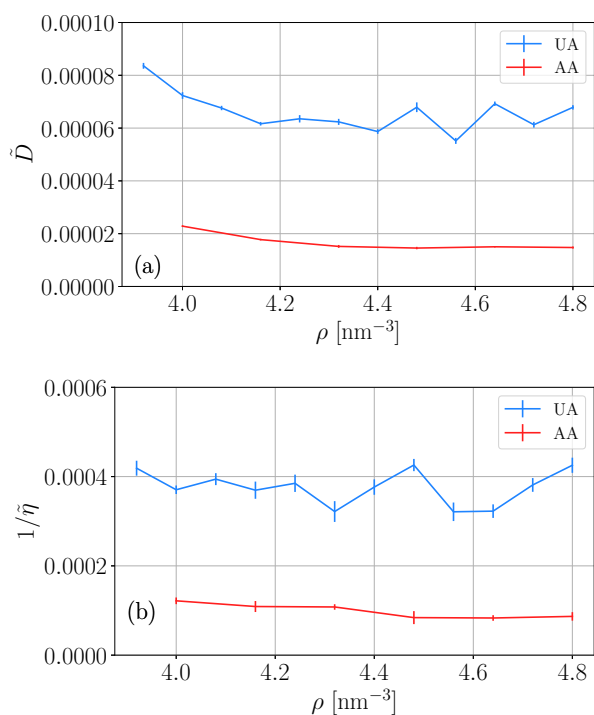


Figure 12. Comparison of dynamics between the united- (UA) and all-atom (AA) models along isodyne HV in scaled units. (a) Scaled diffusion coefficient for N^+ in the cation, and (b) scaled inverse viscosity (fluidity).

of the reduced diffusion coefficient and viscosity along the simulated isodynes. The resulting curves are reasonably flat, which confirms the validity of the procedure for determining the contours. The visible variations are larger than the statistical errors, though, which may result from the uncertainties in locating precisely the isodynes from the fitting process. We have seen that the density scaling exponent of our united-atom model is larger than the value determined experimentally for this IL. A possible reason is the effect of the hydrogen atoms on the temperature dependence of the dynamics. To test for such differences we have carried out a limited number of simulations of an all-atom (AA) model of the same liquid. Details of the AA model can be found in Ref. 35. Rather than repeating the generation of isodynes from scratch we have simulated the AA along the isodyne points identified for the UA model. The diffusivity and inverse viscosity in reduced units are shown along isodyne HV in Fig. 12, where they are compared to the corresponding data for the UA model. As expected the AA model is slower to evolve, showing lower diffusivity and fluidity by factors of 2-3. The statistical error in the AA data is also smaller allowing a slight downward trend to be discerned. However this trend is consistent with the data for the UA model and the quantities shown do not vary more for the AA model than they do for the UA model. This excludes the absence of H atoms from being a cause of the higher γ in the simulations. To go beyond the scalar quantities \tilde{D} and $\tilde{\eta}$, the time-dependent functions from which they are derived are explored.

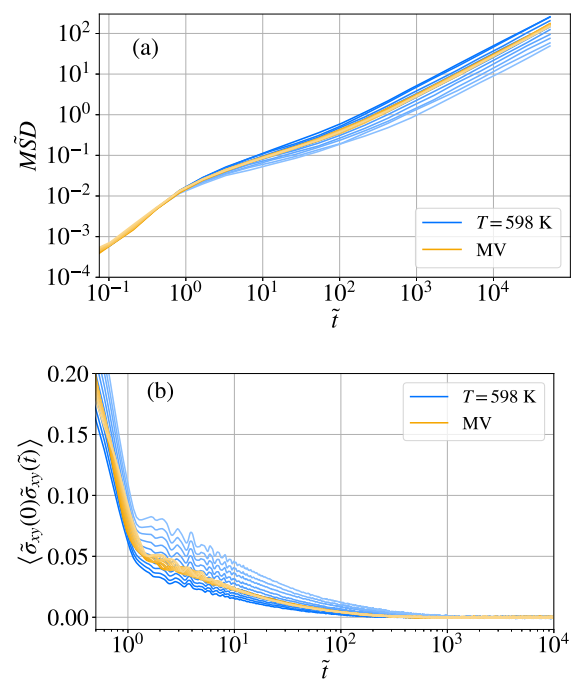


Figure 13. Reduced-unit MSD (a) and stress autocorrelation (b) along isotherm $T = 598$ K (blue curves) and isodyne MV (orange curves).

These include the mean-square displacement (MSD) of N^+ and the shear stress autocorrelation function. These are shown along isodyne MV and the isotherm $T = 598$ K in Fig. 13. There is good collapse for the MSD (panel (a) of the figure), apart from a region at short times where presumably some internal dynamics, not invariant in reduced units, is active. Data for the isotherm $T = 598$ K is shown for comparison. For the stress autocorrelation function (panel (b) of the figure) there is also quite good collapse, particularly when compared to the isothermal data. Some variation is visible at small and intermediate times. In particular the small oscillations at intermediate times 1-10 reduced units vary slightly along the isodyne. In fact in nonreduced units these are aligned in time (data not shown); these are presumably associated with particular internal motions which are not particularly coupled to the overall molecular dynamics and have their own fixed characteristic time scales.

This paper focuses on dynamics rather than structure. Nevertheless, before continuing our investigation of dynamical invariance in the next section with rotational dynamics, it is worth making the point that the curves identified here are *isodynes* rather than *isomorphs*. To this end we show the X-ray structure factor along isodyne MV in Fig. 14(a).

It is clear that the structure is far from invariant. It is also clear that most of the variation is in the low- q "charge-ordering" peak. Indeed, showing $S(q)$ for only two nearby densities, in Fig. 14(b), reveals this contrast more strikingly: for small density changes the main peak is quite invariant while the charge peak changes visibly, becoming smaller and shifting to slightly lower q with increasing density. This is

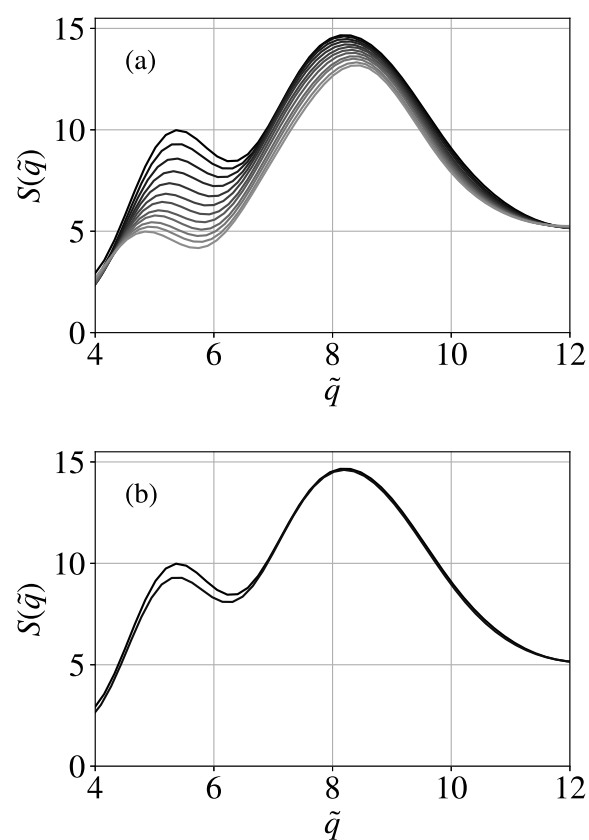


Figure 14. (a) X-ray structure factor along isodyne HV, calculated by Fourier transform of the partial radial distribution functions and summing over all pair types with appropriate weights. Shading is darker for lower densities. (b) Same as (a) but including only the lowest two densities, 3.92 nm^{-3} and 4.0 nm^{-3} , differing by 2%.

668 precisely what has been observed experimentally for this ionic
 669 liquid³⁴. The overall point of Fig. 14, however, is that the
 670 structure varies substantially along a curve on which dynam-
 671 ics is rather invariant. Further examples of structural variation
 672 along isodynes can be found in Ref. 35, where no aspect of
 673 the structure could be identified which is as invariant as the
 674 dynamics. This is a strange situation, since it is a paradigm
 675 in material physics that structure determines dynamics, or at
 676 least plays a crucial role. For example, a well-known theory
 677 for viscous liquid dynamics, mode-coupling theory, is based
 678 entirely on this premise.^{84,85}

679 G. Orientational dynamics along isodynes

680 To widen the scope of dynamical measures encompassed
 681 by isodynes we study other measures of dynamics, specifi-
 682 cally molecular rotations. This is done by defining a normal-
 683 ized vector $\mathbf{e}(t)$ in terms of the atoms within a given molecule
 684 and calculating the time autocorrelation function $P_1(t)$ as the
 685 average dot product of this vector with itself at different times:

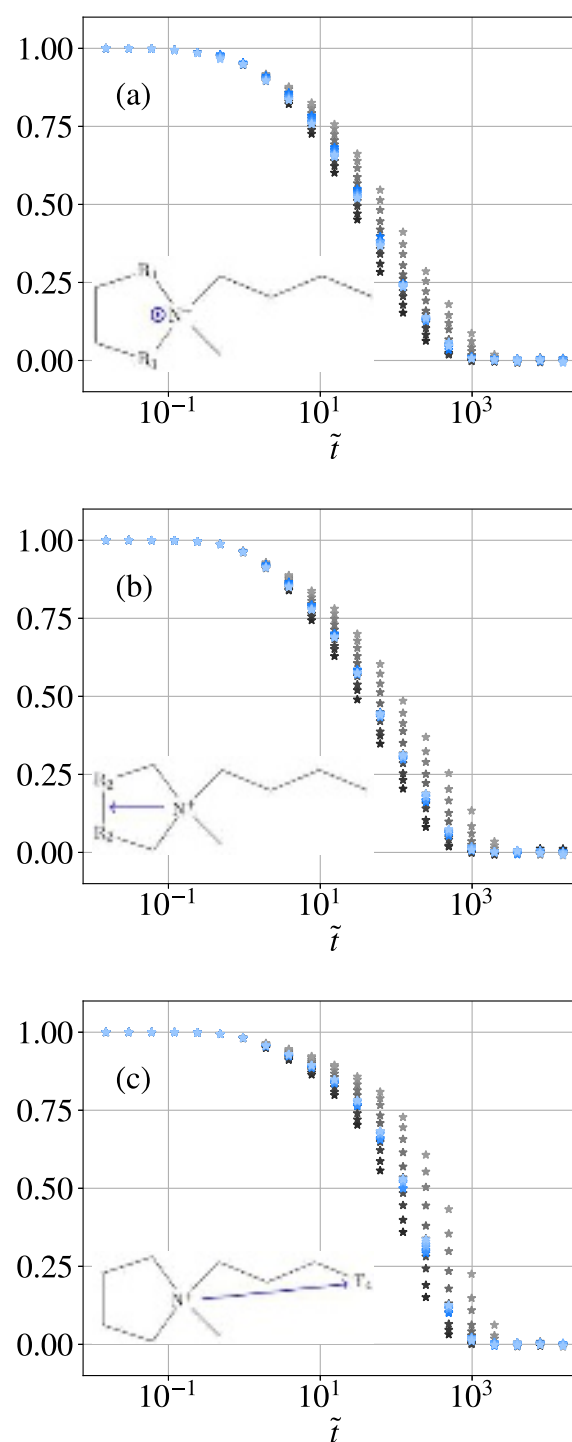


Figure 15. Orientational dynamics of the cation along isodyne MV, shown in different shades of blue for different densities, together with the same function on the isotherm $T=598 \text{ K}$, shown in grey, for more or less the same range of densities. The autocorrelation function of (a) the normal vector to the plane spanned from the two R_1 groups and N^+ , and (b) the vector from N^+ to the point between the two R_2 groups, and (c) the vector from N^+ to the end of the tail (T_4).

$$P_1(t) \equiv \langle \vec{v}(t_0) \cdot \vec{v}(t_0 + t) \rangle. \quad (8)$$

Here the notation P_1 refers to the $l = 1$ Legendre polynomial. Borodin and Smith defined rotational correlation functions more or less similarly in their study of a simulated Pyr13-TFSI ionic liquid, including also $P_2(t)$ functions.⁸⁶ They were interested in the degree of anisotropy, i.e. differences in relaxation rates between rotations in different directions, and found, not surprisingly, that rotations of vectors aligned with the long axes of the ions are slowest. Our primary concern is the degree of invariance along isodynes and whether this varies for different rotations. It should be noted that a rotational correlation function defined in this way is sensitive to two components of rotation, namely rotations about any two axes orthogonal to the given vector. Obviously, rotations about the given vector itself cannot decorrelate it. Starting with the cation, we define three vectors as (a) normal to the plane containing N^+ and the two R_1 groups, (b) the vector from N^+ to the point midway between the two R_1 groups, and (c), the vector from N^+ to the end of the tail T_4 . The two first vectors are meant to test the rotation of the ring, while the latter is meant to test the rotation of the tail. The corresponding $P_1(t)$ correlation functions are shown in Fig. 15 (a), (b) and (c), respectively, along with molecular diagrams indicating the vectors, in the insets. Data for the different state points along the isodyne MV are shown as blue points, while for comparison data along the isotherm $T = 598$ K are shown in grey. All three correlation functions show invariance, such that the different blue data sets cannot be distinguished. By comparison the grey isotherm data are spread out, decaying over a broad range of time scales. The overall shapes of the three correlation functions on the isodyne are similar, showing an emergent two-step appearance, and with the relaxation time increasing somewhat from (a) to (b) to (c). The degree of invariance is greatest for part (b); for the other two functions the blue data points show a small degree of spreading.

For the anion we consider two vectors: (a), the vector from one S atoms to the other (due to the molecule's symmetry the order is irrelevant), and (b) second the normal to the plane containing N^- and the two S atoms. The correlation functions are shown in Fig. 16 (a) and (b), respectively, again from isodyne MV (blue points) and from isotherm $T = 598$ K (grey points). The isodyne data in panel (a) show reasonable invariance, i.e. collapse, although not as striking as that of the cation rotations in Fig. 15). On the other hand, the data in panel (b) vary rather more along the isodyne. In fact the amount of variation is almost comparable to that along the isotherm. This is a striking and noteworthy result: while most of the rotational correlation functions we have investigated show invariance, one does not. The vector involved in the non-invariant rotation is sensitive both to rotations of the anion about its long axis, and to one rotation perpendicular to the long axis. The non-invariant behavior must arise from rotations about the long axis, otherwise it would also be manifested in the other correlation function (panel (a)).

The molecular rotations which show invariance are some how connected to the other dynamical properties showing in

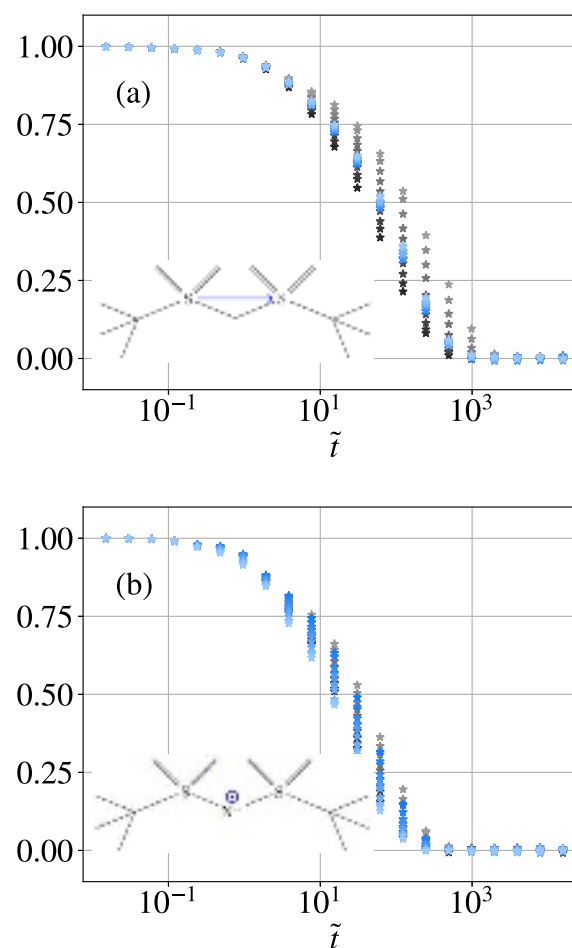


Figure 16. Orientational dynamics of the anion along isodyne MV. The autocorrelation function of (a) the vector between the two S atoms in the anion, and (b) the normal vector to the plane spun from the two S atoms and N^- .

variance along the isodynes, while the rotation which does not must be somehow decoupled from the others and from the other invariant dynamical quantities. From the results of this subsection we see that the rotations associated with a high moment of inertia are invariant, while the case of non-invariant rotational dynamics involves a low moment of inertia (the long axis of the TFSI anion). This is plausible when considering a molecule's interactions with its neighbors. A rotation with high moment of inertia would be more likely to be geometrically constrained by interactions with neighbouring molecules than one with low moment of inertia. Indeed, it makes sense that a molecule can rotate more freely about an axis of low moment of inertia without influencing the overall dynamics of the system. The connection between these observations and the other invariant aspects of the dynamics will be discussed below in the context of coarse-graining.

757 **V. DISCUSSION**758 **A. Significance of Isodynes**

759 How widespread is the existence of isodynes? In an ex-
 760 tensive study,^{87–95} Assael, Dymond and coworkers analyzed
 761 experimental data of the transport coefficients (coefficients of
 762 self-diffusion, viscosity and thermal conductivity) for a wide
 763 range of liquids (see also Ref. 4). They found correlations
 764 between them inspired by the hard spheres model but which
 765 are consistent with isomorph theory. In their approach the
 766 reduced unit form of the transport coefficient is a function
 767 of the molecular volume V scaled by a limiting high density
 768 reference value $V_0(T)$, where the latter is temperature depen-
 769 dent but does not depend on the quantity in question. This is
 770 similar, indeed essentially equivalent to the isomorph-based
 771 analysis by Costigliola *et al.*⁹⁶ where the reduced transport
 772 coefficients are functions of $T/T_{\text{ref}}(\rho)$ (i.e. using ρ , equiva-
 773 lently volume, as the parameter for the reference temperature
 774 instead of the other way around). Indeed the Lennard-Jones
 775 data for $V_0(T)$ presented by Dymond⁶⁷ is consistent with the
 776 latter function being an isomorph—a power-law fit of T ver-
 777 sus $1/V_0$ gives a good fit with exponent close to 6, consis-
 778 tent with density-scaling exponents for LJ systems determined
 779 in isomorph studies.¹⁷ The systems studied by Assael *et al.*
 780 include alkanes,⁸⁷ simple organic molecules,⁸⁸ mixtures of
 781 n -alkanes,⁸⁹ n -alcohols,⁹² refrigerants,⁹³ and more recently,
 782 ionic liquids.⁹⁵ In fact their analysis is not just consistent with
 783 isomorph theory but shows the existence of isodynes—curves
 784 (in their formalism, curves along which the "reduced molar
 785 volume" $V_r \equiv V/V_0(T)$ is constant) along which three trans-
 786 port quantities are invariant in reduced units. This work con-
 787 stitutes a large body of experimental evidence for isodynes.
 788 The theoretical basis for their analysis is the hard-sphere
 789 model for which the transport coefficients are known, and ap-
 790 propriate adjustment factors to account for the non-spherical
 791 nature of the molecules.

792 The important conclusion from the work of Dymond *et al.*
 793 is that the transport coefficients can be invariant on scaling
 794 with isomorph units without any reference to structural scal-
 795 ing (i.e. isomorph behavior), and therefore isodynes may be
 796 more prevalent than isomorphs, and it is perhaps isomorphs
 797 that are, in fact, the exception rather than the rule outside the
 798 domain of model systems, such as Lennard-Jones. Also re-
 799 cent papers by Khrapak and Khrapak^{38,39} indicate that one
 800 can have isodynes without isomorphs in the context reference
 801 density scaling, which is observed at low and medium densi-
 802 ties (see also Ref. 40). The relatively recent investigations of
 803 viscuits (single trajectory contributions to the viscosity) also
 804 suggest that there is an underlying common invariance to the
 805 factors that determine the values of the transport coefficients
 806 which is insensitive to state point.^{97–100}

807 The discovery of isodynes can be viewed as opening a way
 808 to generalize isomorph theory. Apart from isomorphs a nat-
 809 ural framework is Rosenfeld excess entropy scaling,⁶⁶ while
 810 another generalization of the isomorph concept for molecu-
 811 lar systems introduced the term pseudo-isomorphs.¹⁰¹ Rosen-
 812 feld's excess-entropy scaling has recently been reviewed by

813 Dyre⁴⁵, and has typically concerned the three properties vis-
 814 cosity, self-diffusion and thermal conductivity, whose values
 815 in reduced units are fixed by the excess entropy

$$S_{ex} \equiv S(\rho, T) - S_{id}(\rho, T), \quad (9)$$

where S is the full entropy and S_{id} the entropy of the ideal gas
 at the same density and temperature. Excess-entropy scaling
 can be justified if a system can be mapped either to a hard-
 sphere system or to an inverse power law system, but neither
 of these seems plausible in the case of a complex molecular
 system such as the one studied here. There is no consensus
 as to the origin of excess-entropy scaling; clearly it follows
 when there are exact or approximate isomorphs, such that both
 structure and dynamics are invariant in reduced units along
 curves of constant excess entropy (configurational adiabats).
 However, liquids involving flexible molecules can have iso-
 morphs which are not strictly configurational adiabats. The
 contribution to excess entropy from flexible bonds, for exam-
 ple, is decoupled from the invariant dynamics and structure.
 In some simple cases isomorphs can be generated by remov-
 ing the bond dynamics according to a preset procedure.¹⁰¹
 The resulting isomorphs are termed "pseudo-isomorphs" to
 emphasize that they are not configurational adiabats. More-
 over atomic systems with charge can exhibit invariant dynam-
 ics but not invariant structure on configurational adiabats.³⁶
 In fact, considering the three types of invariant quantity, the
 following situations may be considered,

- A:** invariant structure (full or partial)
- B:** invariant dynamics (full or partial)
- C:** Correspondance of A or B with invariant excess entropy

We can identify systems with all three characteristics (true
 isomorphs), just A and B (pseudoisomorphs), just B and C
 (simple ionic liquids, excess entropy scaling), or just B (com-
 plex ionic and small molecule liquids). In particular iso-
 morphs constitute a special case of isodynes, while excess
 entropy scaling and isodynes both constitute generalizations.
 The underlying connection between these related concepts
 is as yet unclear: Dyre concluded that "it remains an open
 question whether all aspects of excess-entropy scaling and re-
 lated regularities reflect hidden scale invariance in one form
 or other";⁴⁵ this question remains open, and we believe that
 isodynes are part of the resolution of this issue. A theoretical
 framework is required to unify these different combinations.
 It is likely that coarse-graining, to be discussed in the next
 section, has a key role to play.

B. Coarse-graining

Coarse-graining, the simplification of a model system by
 removing some of the degrees of freedom, is often presented
 as a practical tool to increase the time scales of simulations;

a natural requirement is that the overall dynamics of the remaining degrees of freedom be preserved (apart from a possible rescaling of time: typically the coarse grained system intrinsically evolves faster than the original⁴⁸). But it can also be a conceptual tool, to understand how simplicity emerges in complex systems when irrelevant microscopic degrees of freedom are ignored. Ideally one should be able to identify an analog to the excess entropy which is defined in the coarse-grained system and whose contours coincide with the isodynes. The fact that for our two models, united-atom and all-atom, where the former can be understood as a coarse-graining of the latter, share isodynes is encouraging in this respect. In fact we suggest that preservation of isodynes, where they exist, should be a requirement of any reliable coarse-graining procedure.

Our results can be encapsulated by the statement that the "coarse-grained dynamics are simple". The coarse-grained dynamics includes the dynamical quantities that are defined for a suitably coarse-grained model such as, shear-viscosity, self-diffusion, and most molecular rotations. In other words, these are *intermolecular* dynamics, but not *intramolecular* dynamics (which is largely decoupled from isodynes). "Simple" means that isodynes exist, in effect making the phase diagram one-dimensional as far as dynamics is concerned. The molecular rotations which are not invariant on isodynes, i.e., are decoupled from isodynes, can be characterized as those with lower moments of inertia, for example a rotation about the long axis of TFSI, Fig. 16(b). But it is not the moment of inertia itself that is relevant; it is more that such rotations disappear as degrees of freedom under sufficient coarse graining under which for example TFSI would be represented as a cylinder with rounded ends.

Another example of the distinction between invariant CG degrees of freedom and decoupled intra-molecular degrees of freedom turns up in the stress autocorrelation function, whose overall decay is quite invariant along isodynes, but in which the small wiggles, presumably associated with intra-molecular degrees of freedom, are not.

However just as coarse-graining, as a simulation technique, does not in practice guarantee faithful reproduction of dynamics,^{102,103} as a conceptual tool it is not guaranteed that a simple entropy-like quantity characterizing isodynes can be identified. Moreover, coarse-graining would not seem to be able to explain the case of simple ionic liquids which have isodynes but not isomorphs, since there are no obvious degrees of freedom that could be removed. Coarse-graining a complex ionic liquid would still leave the charge-ordering unaffected, an aspect of structure that is not invariant.

We consider that a carefully designed CG model could in principle illuminate the phenomenon of isodynes. It is significant that the AA version of our model seems to have essentially the same isodynes as the UA model. But there is a question of how to guarantee this feature if one were to develop a more coarse-grained model than the UA one. One proposal in the literature, based on the concept of relative entropy addresses more or less explicitly the slope of isodynes by coarse-graining to soft-sphere systems (inverse power-law potentials).¹⁰⁴ Ideally one would not explicitly tar-

get the shapes of isodynes, but identify some structural property whose consistency from AA to UA to CG would ensure the consistency of the isodynes; in that case one could claim to have understood the presence of the latter in the more fine grained models. In fact, preserving the location of isodynes could be a useful criterion for confirming dynamical consistency for between the AA and CG models.

VI. SUMMARY AND PERSPECTIVES

The main results of this work can be summarized as follows:

1. For these model ionic liquids, there exists a set of curves, termed isodynes, along which a number of dynamical quantities are invariant, even though there are no isomorphs for these systems.
2. The curves $T(\rho)$ along an isodyne can be well fitted by an exponential form, which corresponds to a density scaling exponent, γ , which increases with increasing density along a given isodyne. When considering the overall picture of how γ varies in the phase diagram, however, it depends more on temperature than on density (Fig. 8(b)).
3. The quantities that have been tested and shown to be (approximately) invariant are: viscosity, the stress autocorrelation function, the mean squared displacement and the diffusion coefficient, and several rotational correlation functions. Of these, three are associated with cation rotations and one with anion rotation.
4. One tested anion rotational correlation function was not invariant. This is sensitive to rotations about the "long axis" of the molecule. A consequence of this lack of invariance is that this motion is not very important for, and is largely decoupled from, the general behavior of the liquid and could be "coarse-grained away".

We are far from having exhausted the possibilities for studying dynamical invariances in this IL system. With the exception of viscosity and the stress-autocorrelation function, our analyses pertained only to single-molecule dynamical properties. A natural next step would be to investigate correlated motion of ions. One issue is the existence of ion-pairs.²² Correlations are particularly important in the context of the electrical conductivity, where they lead to departures from the Nernst-Einstein relation,^{73,105} according to which the electrical conductivity is determined by the diffusivities of the ions without regard to correlations. Furthermore it is plausible that correlations are strongly affected by Coulomb interactions, and thus might be a dynamical feature which varies along isodynes, i.e. an exception to dynamical invariance.

Regarding the relation between isodynes and coarse-graining, the role of charges seems to be separate from that of intra-molecular degrees of freedom. Work on non-charged, but otherwise complex and flexible, molecular systems will also be necessary to better clarify this. To summarize, it is

clear from this work that molecular simulation will continue to be an important tool in helping to understand and characterize these complex charged molecular systems, and in particular the identification of isodynes, done here for the first time, will be relevant for providing guidelines for designing practical applications involving them.

VII. SUPPLEMENTAL MATERIAL

The supplemental material contains further details of the model and force field including tables of parameters, a description of our approach to handling Coulomb forces, tests relating to cutoffs, details relating to the analysis, and additional data for rotational correlations.

ACKNOWLEDGMENTS

We thank Dr. Lorenzo Costigliola (Roskilde University, Denmark) for helpful discussions. Funding from the Danish Ministry of Higher Education and Science through the ESS SMART Lighthouse is gratefully acknowledged. D.D. acknowledges the Royal Academy of Engineering for funding his Shell/RAEng Research Chair in Complex Engineering Interfaces and the EPSRC for the Prosperity Partnership EP/V038044/1. D.D. and D.M.H. acknowledge the support received from the EPSRC under the Established Career Fellowship Grant No. EP/N025954/1.

VIII. DATA AVAILABILITY

Scripts and data files sufficient to generate the figures of the manuscript, as well as the python scripts for running the simulations themselves have been uploaded to Zenodo.

REFERENCES

- A. Tölle, H. Schober, J. Wuttke, O. Randl, and F. Fujara, *Phys. Rev. Lett.* **80**, 2374 (1998).
- C. Alba-Simionesco, A. Cailliaux, A. Alegria, and G. Tarjus, *Europhys. Lett.* **68**, 58 (2004).
- R. Casalini and C. M. Roland, *Phys. Rev. E* **69**, 062501 (2004).
- J. Millat, J. H. Dymond, and C. A. Nieto de Castro, eds., *Transport Properties of Fluids: Their Correlation, Prediction and Estimation* (Cambridge University Press, 1996), ISBN 978-0-521-46178-8.
- C. M. Roland, S. Hensel-Bielowka, M. Paluch, and R. Casalini, *Rep. Prog. Phys.* **68**, 1405 (2005).
- K. Niss and T. Hecksher, *J. Chem. Phys.* **149**, 230901 (2018).
- K. L. Ngai, R. Casalini, S. Capaccioli, M. Paluch, and C. M. Roland, *Journal of Physical Chemistry B* **109**, 17356 (2005).
- K. Adrjanowicz, J. Pionteck, and M. Paluch, *RSC Adv.* **6**, 49370 (2016).
- K. Ngai and M. Paluch, *Journal of Non-Crystalline Solids* **478**, 1 (2017).
- H. W. Hansen, A. Sanz, K. Adrjanowicz, B. Frick, and K. Niss, *Nat. Commun.* **9**, 518 (2018).
- H. W. Hansen, B. Frick, S. Capaccioli, A. Sanz, and K. Niss, *The Journal of Chemical Physics* **149**, 214503 (2018).
- N. Gnan, T. B. Schröder, U. R. Pedersen, N. P. Bailey, and J. C. Dyre, *J. Chem. Phys.* **131**, 234504 (2009), <https://doi.org/10.1063/1.3265957>.
- T. B. Schröder and J. C. Dyre, *J. Chem. Phys.* **141**, 204502 (2014).
- J. C. Dyre, *J. Phys. Chem. B* **118**, 10007 (2014), pMID: 25011702, <https://doi.org/10.1021/jp501852b>.
- C. M. Roland, *Macromolecules* **43**, 7875 (2010).
- F. Hummel, G. Kresse, J. C. Dyre, and U. R. Pedersen, *Phys. Rev. B* **92**, 174116 (2015).
- N. P. Bailey, U. R. Pedersen, N. Gnan, T. B. Schröder, and J. C. Dyre, *J. Chem. Phys.* **129**, 184507 (2008).
- T. B. Schröder, N. P. Bailey, U. R. Pedersen, N. Gnan, and J. C. Dyre, *J. Chem. Phys.* **131**, 234503 (2009).
- S. Pawlus, M. Paluch, J. Ziolo, and C. M. Roland, *Journal of Physics: Condensed Matter* **21**, 332101 (2009).
- L. A. Roed, D. Gundermann, J. C. Dyre, and K. Niss, *J. Chem. Phys.* **139**, 101101 (2013).
- M. Romanini, M. Barrio, R. Macovez, M. D. Ruiz-Martin, S. Capaccioli, and J. L. Tamarit, *Scientific Reports* **7**, 1346 (2017), ISSN 2045-2322.
- Y.-L. Wang, B. Li, S. Sarman, F. Mocci, Z.-Y. Lu, J. Yuan, A. Laaksonen, and M. D. Fayer, *Chem. Rev.* **120**, 5798 (2020).
- C. M. Roland, S. Bair, and R. Casalini, *J. Chem. Phys.* **125**, 124508 (2006).
- A. S. Pensado, A. A. H. Pádua, M. J. P. Comuñas, and J. Fernández, *J. Phys. Chem. B* **112**, 5563 (2008).
- M. Paluch, S. Haracz, A. Grzybowski, M. Mierzwa, J. Pionteck, A. Rivera-Calzada, and C. Leon, *J. Phys. Chem. Lett.* **1**, 987 (2010).
- E. R. López, A. S. Pensado, M. J. Comuñas, A. A. Pádua, J. Fernández, and K. R. Harris, *J. Chem. Phys.* **134**, 144507 (2011).
- M. Paluch, E. Masiewicz, A. Grzybowski, S. Pawlus, J. Pionteck, and Z. Wojnarowska, *J. Chem. Phys.* **141**, 134507 (2014).
- Z. Wojnarowska, G. Jarosz, A. Grzybowski, J. Pionteck, J. Jacquemin, and M. Paluch, *Phys. Chem. Chem. Phys.* **16**, 20444 (2014).
- K. R. Harris and M. Kanakubo, *Phys. Chem. Chem. Phys.* **17**, 23977 (2015).
- M. Paluch, Z. Wojnarowska, P. Goodrich, J. Jacquemin, J. Pionteck, and S. Hensel-Bielowka, *Soft Matter* **11**, 6520 (2015).
- Z. Wojnarowska, L. Tajber, and M. Paluch, *J. Phys. Chem. B* **123**, 1156 (2019).
- K. R. Harris and M. Kanakubo, *Phys. Chem. Chem. Phys.* **24**, 14430 (2022).
- K. R. Harris, M. Kanakubo, D. Kodama, T. Makino, Y. Mizuguchi, Y. Suzuki, and T. Watanabe, *Journal of Chemical & Engineering Data* **68**, 549 (2023), ISSN 0021-9568, URL <https://doi.org/10.1021/acs.jced.2c00713>.
- H. W. Hansen, F. Lundin, K. Adrjanowicz, B. Frick, A. Matic, and K. Niss, *Phys. Chem. Chem. Phys.* **22**, 14169 (2020).
- P. A. Knudsen, Ph.D. thesis, Roskilde University (2022).
- P. A. Knudsen, K. Niss, and N. P. Bailey, *J. Chem. Phys.* **155**, 054506 (2021).
- I. H. Bell, R. Fingerhut, J. Vrabec, and L. Costigliola, *J. Chem. Phys.* **157**, 074501 (2022).
- S. A. Khrapak and A. G. Khrapak, *Phys. Rev. E* **103**, 042122 (2021).
- S. A. Khrapak and A. G. Khrapak, *The Journal of Physical Chemistry Letters* **13**, 2674 (2022), pMID: 35302377.
- D. M. Heyes, D. Dini, S. Pieprzyk, and A. C. Brańka, *The Journal of Chemical Physics* **158**, 134502 (2023).
- T. B. Schröder, U. R. Pedersen, N. P. Bailey, S. Toxvaerd, and J. C. Dyre, *Phys. Rev. E* **80**, 041502 (2009).
- L. V. Woodcock, *Proceedings of the Royal Society of London, Series A* **348**, 187 (1976).
- J. M. Young, I. H. Bell, and A. H. Harvey, *J. Chem. Phys.* **158**, 024502 (2023).
- R. Macías-Salinas and J. Gross, *Fluid Phase Equilib.* **574**, 113897 (2023).
- J. C. Dyre, *J. Chem. Phys.* **149**, 210901 (2018).
- A. Saliou, P. Jarry, and N. Jakse, *Phys. Rev. E* **104**, 044128 (2021).
- J. Jin, K. S. Schweizer, and G. A. Voth (2022), [arxiv/2208.00078](https://arxiv.org/abs/2208.00078).
- J. P. Ewen, C. Gattinoni, F. M. Thakkar, N. Morgan, H. A. Spikes, and D. Dini, *Materials (Basel)* **9**, 651 (2016).
- W. L. Jorgensen, J. Chandrasekhar, J. D. Madura, R. W. Impey, and M. L. Klein, *The Journal of Chemical Physics* **79**, 926 (1983), <https://doi.org/10.1063/1.445869>.
- W. L. Jorgensen and J. Tirado-Rives, *Journal of the American Chemical Society* **110**, 1657 (1988), pMID: 27557051.

This is the author's peer reviewed, accepted manuscript. However, the online version of record will be different from this version once it has been copyedited and typeset.

PLEASE CITE THIS ARTICLE AS DOI: 10.1063/5.0177373

- 1089 ⁵¹W. L. Jorgensen, D. S. Maxwell, and J. Tirado-Rives, *Journal of the American Chemical Society* **118**, 11225 (1996). 1138
- 1090
- 1091 ⁵²S. V. Sambasivarao and O. Acevedo, *Journal of Chemical Theory and Computation* **5**, 1038 (2009), pMID: 26609613, <https://doi.org/10.1021/ct900009a>. 1141
- 1092
- 1093
- 1094 ⁵³B. Doherty, X. Zhong, S. Gathiaka, B. Li, and O. Acevedo, *Journal of Chemical Theory and Computation* **13**, 6131 (2017), pMID: 29112809, <https://doi.org/10.1021/acs.jctc.7b00520>. 1144
- 1095
- 1096 ⁵⁴J. N. Canongia Lopes and A. A. H. Pádua, *The Journal of Physical Chemistry B* **108**, 16893 (2004), <https://doi.org/10.1021/jp0476545>. 1146
- 1097
- 1098 ⁵⁵H. Xing, X. Zhao, Q. Yang, B. Su, Z. Bao, Y. Yang, and Q. Ren, *Industrial & Engineering Chemistry Research* **52**, 9308 (2013), <https://doi.org/10.1021/ie400999f>. 1149
- 1099
- 1100
- 1101 ⁵⁶W. D. Cornell, P. Cieplak, C. I. Bayly, I. R. Gould, K. M. Merz, D. M. Ferguson, D. C. Spellmeyer, T. Fox, J. W. Caldwell, and P. A. Kollman, *Journal of the American Chemical Society* **118**, 2309 (1996). 1152
- 1102
- 1103 ⁵⁷Z. Liu, S. Huang, and W. Wang, *The Journal of Physical Chemistry B* **108**, 12978 (2004). 1154
- 1104
- 1105 ⁵⁸W. L. Jorgensen, J. D. Madura, and C. J. Swenson, *Journal of the American Chemical Society* **106**, 6638 (1984), <https://doi.org/10.1021/ja00334a030>. 1156
- 1106
- 1107 ⁵⁹A. M. Smondyrev and M. L. Berkowitz, *Journal of Computational Chemistry* **20**, 531 (1999). 1158
- 1108
- 1109 ⁶⁰A. K. Giri and E. Spohr, *J. Mol. Liq.* **228**, 63 (2017). 1159
- 1110
- 1111 ⁶¹N. Bailey, T. Ingebrigtsen, J. S. Hansen, A. Veldhorst, L. Bøhling, C. Lemarchand, A. Olsen, A. Bacher, L. Costigliola, U. Pedersen, et al., *SciPost Physics* **3** (2017). 1162
- 1112
- 1113 ⁶²C. Xu and Z. Cheng, *Processes (Basel)* **9**, 337 (2021). 1163
- 1114
- 1115 ⁶³J. O. Valderrama, L. A. Forero, and R. E. Rojas, *Ind. Eng. Chem. Res.* **51**, 7838 (2012). 1165
- 1116
- 1117 ⁶⁴K. R. Harris, L. A. Woolf, M. Kanakubo, and T. Rütger, *Journal of Chemical & Engineering Data* **56**, 4672 (2011). 1167
- 1118
- 1119 ⁶⁵J. P. Hansen and I. R. McDonald, *Phys. Rev. A* **11**, 2111 (1975). 1168
- 1120
- 1121 ⁶⁶Y. Rosenfeld, *Phys. Rev. A* **15**, 2545 (1977). 1169
- 1122
- 1123 ⁶⁷J. H. Dymond, *Int. J. Thermophys.* **18**, 303 (1997). 1170
- 1124
- 1125 ⁶⁸Note 1, the contour function in the Matplotlib python library. 1171
- 1126 ⁶⁹A. Z. Panagiotopoulos, *J. Phys. Condens. Matter* **17**, S3205 (2005). 1172
- 1127 ⁷⁰U. Balucani and M. Zoppi, *Dynamics of the liquid state* (Clarendon Press, Oxford, 1994), ISBN 9780198517399. 1174
- 1128 ⁷¹T. Köddermann, R. Ludwig, and D. Paschek, *Chemphyschem* **9**, 1851 (2008). 1175
- 1129 ⁷²M. Kanakubo, K. R. Harris, N. Tsuchihashi, K. Ibuki, and M. Ueno, *J. Phys. Chem. B* **111**, 2062 (2007). 1178
- 1130
- 1131 ⁷³H. Liu and E. Maginn, *J. Chem. Phys.* **135**, 124507 (2011). 1179
- 1132
- 1133 ⁷⁴J. C. Araque, S. K. Yadav, M. Shadeck, M. Maroncelli, and C. J. Margulis, *J. Phys. Chem. B* **119**, 7015 (2015). 1181
- 1134
- 1135 ⁷⁵L. Costigliola, D. M. Heyes, T. B. Schröder, and J. C. Dyre, *The Journal of Chemical Physics* **150**, 021101 (2019). 1183
- 1136 ⁷⁶R. Zwanzig, *The Journal of Chemical Physics* **79**, 4507 (1983). 1184
- 1185
- ⁷⁷R. Zwanzig and A. K. Harrison, *The Journal of Chemical Physics* **83**, 5861 (1985).
- ⁷⁸N. H. March and M. P. Tosi, *Phys. Rev. E* **60**, 2402 (1999).
- ⁷⁹N. H. March and J. A. Alonso, *Phys. Rev. E* **73**, 032201 (2006).
- ⁸⁰J. C. M. Li and P. Chang, *J. Chem. Phys.* **23**, 518 (1955).
- ⁸¹R. E. Meyer and N. H. Nachtrieb, *J. Chem. Phys.* **23**, 1851 (1955).
- ⁸²S. Khrapak and A. Khrapak, *Physical Review E* **104**, 044110 (2021).
- ⁸³S. Khrapak and A. Khrapak, *Journal of Chemical Physics* **158**, 206101 (2023).
- ⁸⁴U. Bengtzelius, W. Götze, and A. Sjölander, *Journal of Physics C: Solid State Physics* **17**, 5915 (1984).
- ⁸⁵W. Götze and L. Sjögren, *Reports on Progress in Physics* **55**, 241 (1992).
- ⁸⁶O. Borodin and G. D. Smith, *J. Phys. Chem. B* **110**, 11481 (2006).
- ⁸⁷M. J. Assael, J. H. Dymond, M. Papadaki, and P. M. Patterson, *Int. J. Thermophys.* **13**, 269 (1992).
- ⁸⁸M. J. Assael, J. H. Dymond, M. Papadaki, and P. M. Patterson, *Fluid Phase Equilib.* **75**, 245 (1992).
- ⁸⁹M. J. Assael, J. H. Dymond, M. Papadaki, and P. M. Patterson, *Int. J. Thermophys.* **13**, 659 (1992).
- ⁹⁰M. J. Assael, J. H. Dymond, and P. M. Patterson, *Int. J. Thermophys.* **13**, 729 (1992).
- ⁹¹M. J. Assael, J. H. Dymond, and P. M. Patterson, *Int. J. Thermophys.* **13**, 895 (1992).
- ⁹²M. J. Assael, J. H. Dymond, and S. K. Polimatidou, *Int. J. Thermophys.* **15**, 189 (1994).
- ⁹³M. J. Assael, J. H. Dymond, and S. K. Polimatidou, *Int. J. Thermophys.* **16**, 761 (1995).
- ⁹⁴M. J. Assael, A. E. Kalyva, K. E. Kakosimos, and K. D. Antoniadis, *Int. J. Thermophys.* **30**, 1733 (2009).
- ⁹⁵F. M. Gaciño, M. J. P. Comuñas, J. Fernández, S. K. Mylona, and M. J. Assael, *Int. J. Thermophys.* **35**, 812 (2014).
- ⁹⁶L. Costigliola, U. R. Pedersen, D. M. Heyes, T. B. Schröder, and J. C. Dyre, *J. Chem. Phys.* **148**, 081101 (2018).
- ⁹⁷D. M. Heyes, E. R. Smith, and D. Dini, *The Journal of Chemical Physics* **150** (2019), ISSN 0021-9606, 174504.
- ⁹⁸D. M. Heyes, D. Dini, and E. R. Smith, *The Journal of Chemical Physics* **152** (2020), ISSN 0021-9606, 194504.
- ⁹⁹D. M. Heyes, D. Dini, and E. R. Smith, *The Journal of Chemical Physics* **154** (2021), ISSN 0021-9606, 074503.
- ¹⁰⁰D. M. Heyes and D. Dini, *The Journal of Chemical Physics* **156** (2022), ISSN 0021-9606, 124501.
- ¹⁰¹A. E. Olsen, J. C. Dyre, and T. B. Schröder, *J. Chem. Phys.* **145**, 241103 (2016).
- ¹⁰²S. Kloth, M. P. Bernhardt, N. F. A. van der Vegt, and M. Vogel, *J. Phys. Condens. Matter* **33**, 204002 (2021).
- ¹⁰³J. F. Rudzinski, S. Kloth, S. Wörner, T. Pal, K. Kremer, T. Bereau, and M. Vogel, *J. Phys. Condens. Matter* **33**, 224001 (2021).
- ¹⁰⁴M. S. Shell, *J. Chem. Phys.* **137**, 084503 (2012).
- ¹⁰⁵A. Afandak and H. Eslami, *J. Phys. Chem. B* **121**, 7699 (2017).